Supporting Information

Compact Superlattice as Label-free Surface-Enhanced Raman Scattering Substrate for Noninvasive Urine Test in the Diagnosis of Lung Cancer

Kaili Zhang, ‡[a] Yuancai Ge, ‡[b] Yi Xu, [d] Yujie Liu, [b] Chaoyue Cui, [b] Yuxin Liang, [b] Yangxuan Lin, [e] Jungeng Zhang, [e] Qingwen Zhang, *[c] Yi Wang, *[b,a,c] Xiaoming Lin*[e]

a School of Opto-Electronic Engineering, Changchun University of Science and Technology, Changchun, 130022, China.

b School of Biomedical Engineering, School of Ophthalmology & Optometry, Wenzhou Medical University, Wenzhou, 325027, China.

c Wenzhou Institute, University of Chinese Academy of Sciences, Wenzhou, 325001, China.

d School of Optoelectronic Engineering, Guilin University of Electronic Technology, Guilin 541004, China.

e Department of Thoracic Surgery, the First Affiliated Hospital of Wenzhou Medical University, Wenzhou, 325000, China.

† Electronic supplementary information (ESI) available. See DOI:

‡ These authors contributed equally to this work.

∗ Corresponding authors: Qingwen Zhang, Yi Wang, Xiaoming Lin

E-mail address: zhangqw@wiucas.ac.cn(Q. Zhang), yiwang@wmu.edu.cn(Y. Wang), linxiaoming@wmu.edu.cn(X. Lin)

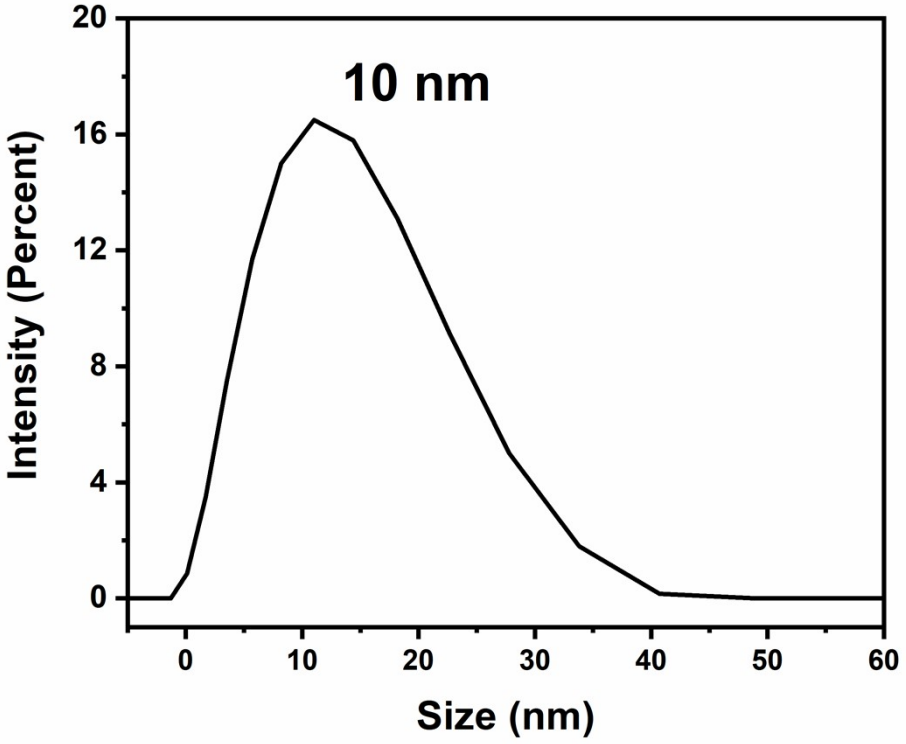

Fig.S1 Dynamic light scattering of the as-prepared Au seeds dispersed in 200 μL DI water.

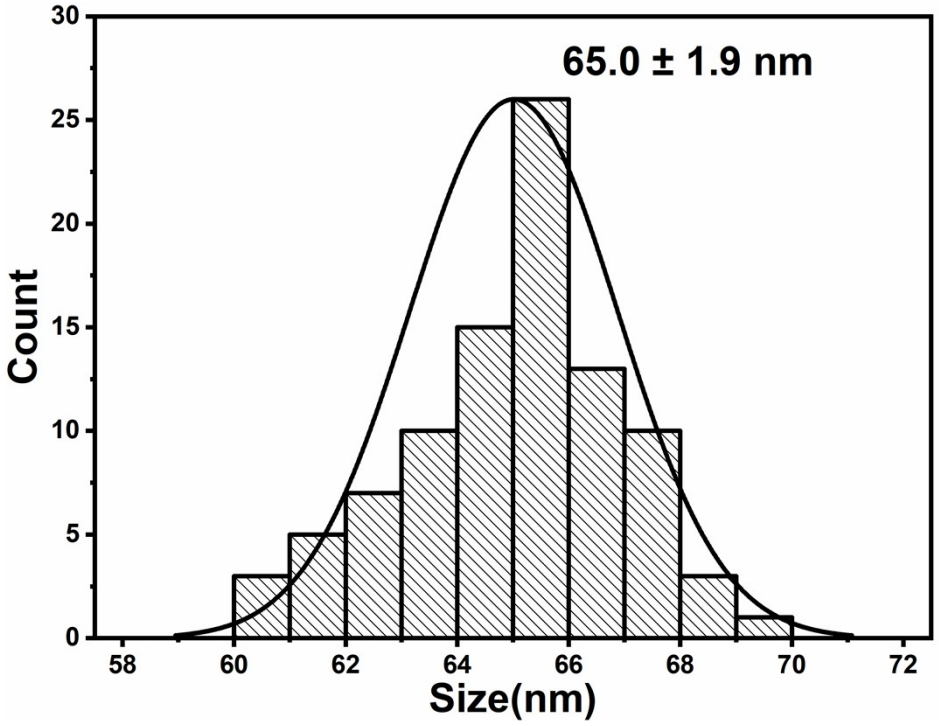

Fig.S2 Histogram of nanoparticle size distribution of the as-prepared Au RDs obtained from SEM images.

The size of the histogram of nanoparticle size distribution (65 nm) is the same as the size observed by TEM and SEM (65 nm).

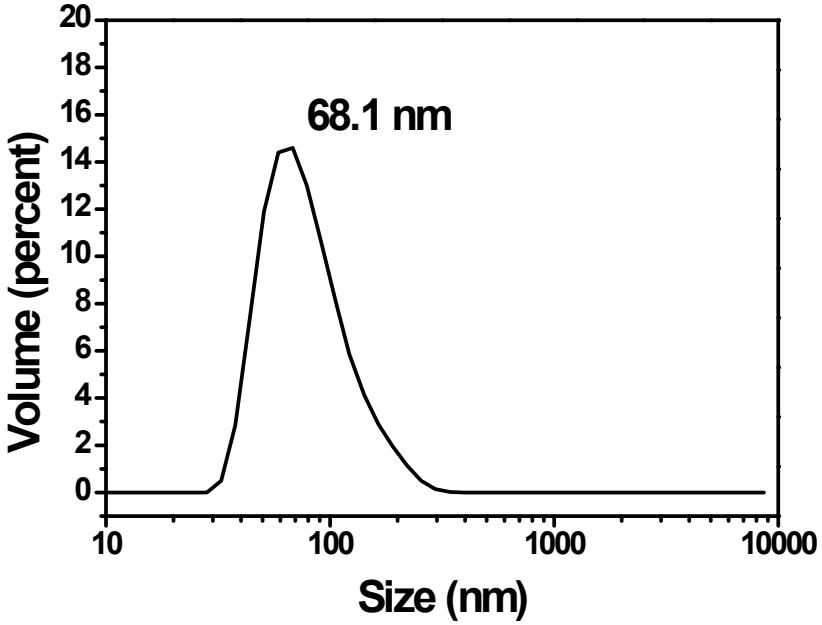

Fig. S3 Dynamic light scattering of the as-prepared Au RDs dispersed in 200 μL DI water. PDI=0.08.

DLS measurement was carried by dissolving 25 μL concentrated Au RD NCs solution in 2.5 mL deionized water and sonicated for 2 min to form a light purple solution. Due to the hydrodynamic interactions, the size (68.1 nm) recorded with DLS is a little larger than the size (65 nm) observed with TEM and SEM.

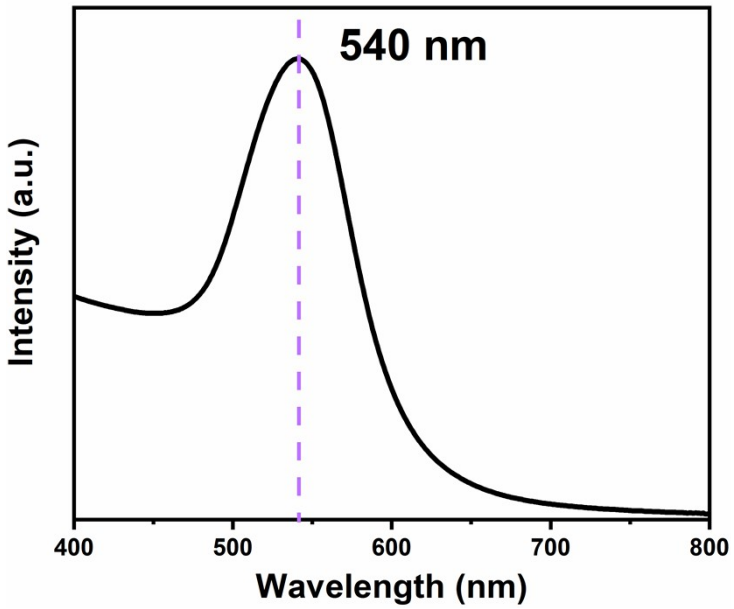

Fig. S4 UV-Vis spectra of the as-prepared Au RDs measured in water.

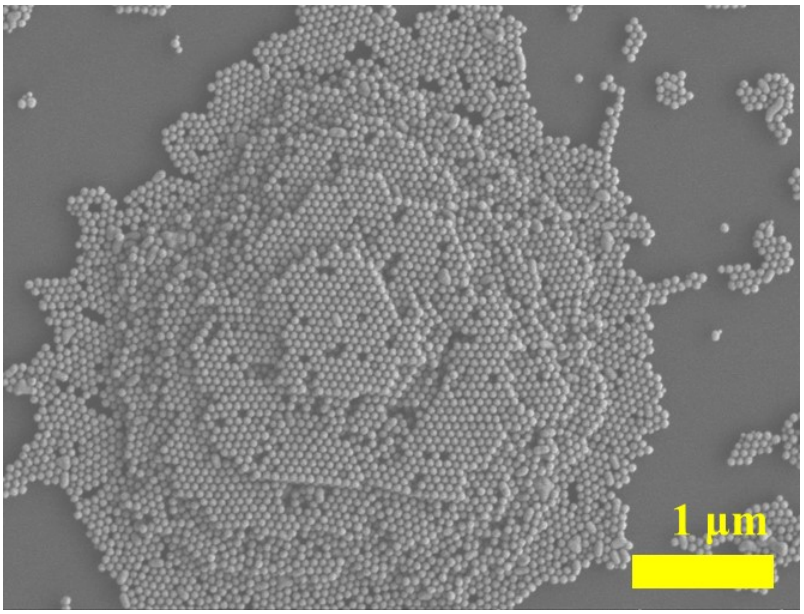

Fig. S5 Au superlattice constructed with Au RDs concentration of 0.5 nM.

By decreasing the concentration of Au RDs solution from 2.75 nM to 0.5 nM, lots of defects can be observed in the central area of the Au superlattice, which may reduce the intensity of the SERS signal. Thus, the superlattice adopted in this study is fabricated by using 2.75 nM Au RDs solution.

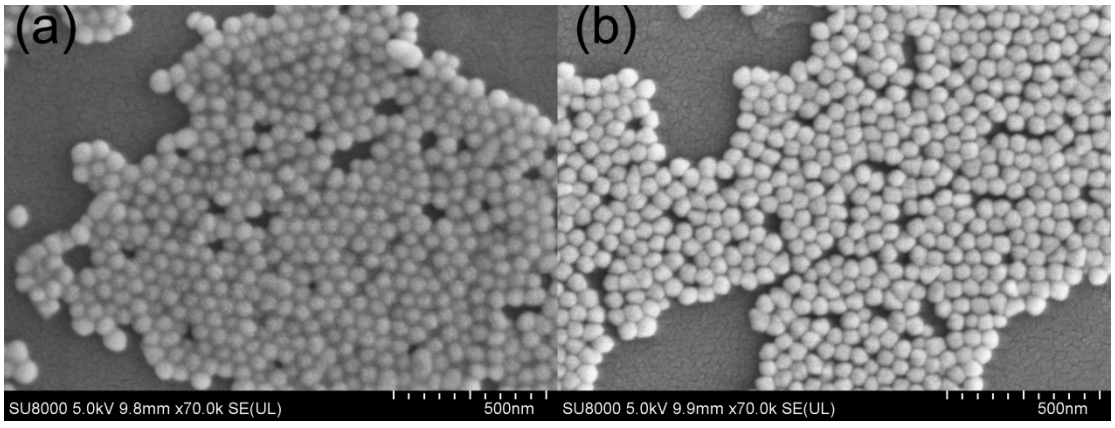

Fig. S6 SEM images of Au RDs before (a) and after (b) plasma treatment.

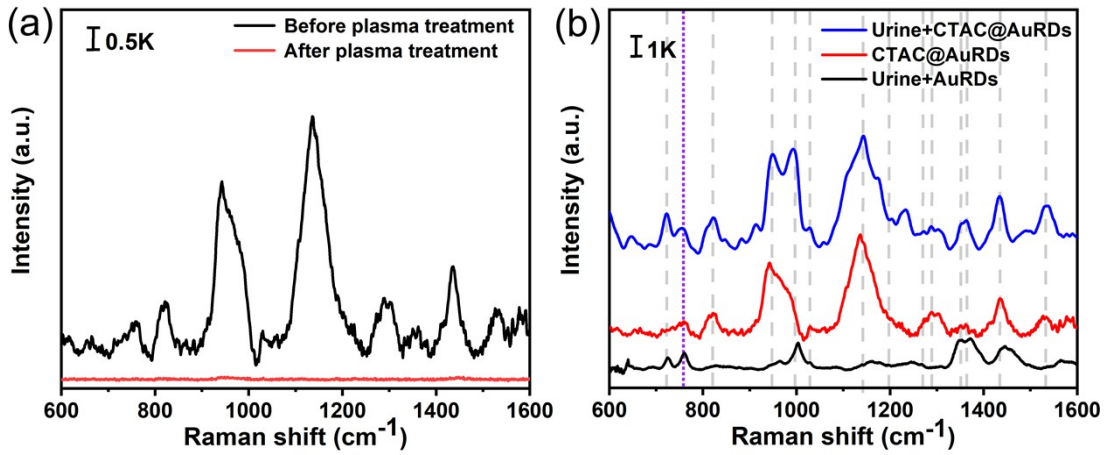

Fig. S7 SERS signals of superlattice before and after treated with plasma for 3 minutes(a), and SERS signals of the untreated superlattice (CTAC@AuRDs) measured with urine samples (urine+CTAC@AuRDs), and plasma treated superlattice measured with urine samples (Urine+AuRDs) (b).

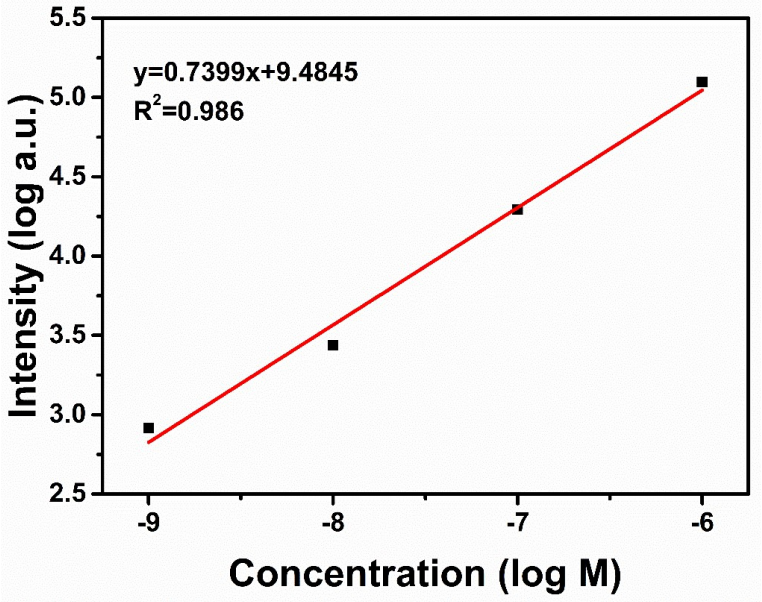

Fig. S8 Linear correlation curve of Raman intensities at 1648 cm^{-1} with the different concentrations of R6G.

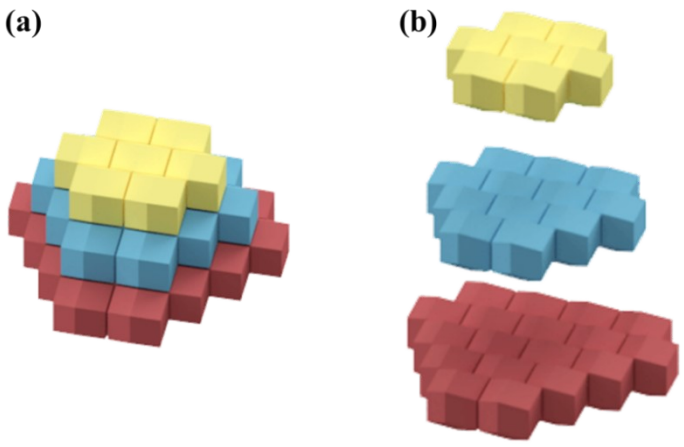

Fig. S9 (a) 3D model of the Au compact superlattice. Each layer of the superlattice is also shown in (b) for a clear view of the compact superlattice.

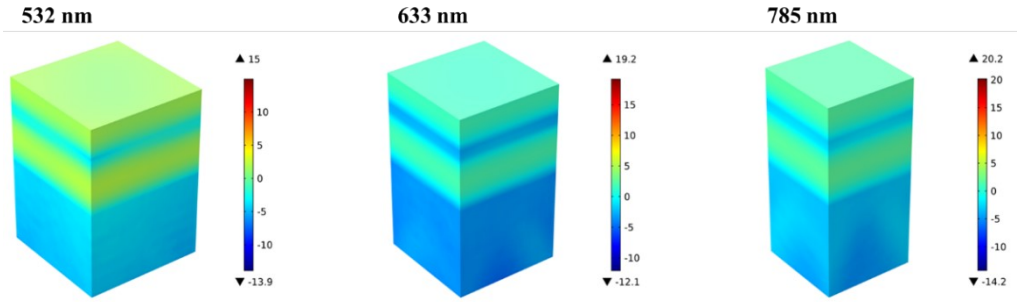

Fig. S10 The distribution of SERS-EF with different excitation wavelengths (532 nm, 633 nm, and 785 nm) in the calculation domain of the numerical simulation.

The enhancement factor (EF) was typically calculated based on the following formula, on case 4-aminothiophene (4-ATP) was used as the probe molecule:

$$EF = (I_{1080\text{-}1}/N_{4\text{-}ATP})/(I_{RS}/N_{RS}).$$

Where $I_{1080cm\text{-}1}$ is the measured SERS intensity of 4-ATP at 1080 cm^{-1}, $N_{4\text{-}ATP}$ is the number of 4-ATP molecules adsorbed on the SERS substrate in each measurement, I_{RS} is the measured Raman intensity of 4-ATP powder at the 1080 cm^{-1} band in a normal Raman spectrum, N_{RS} is the number of 4-ATP molecules measured in the normal Raman measurement without enhancement. Based on the measured SERS intensity, the

average amount of 4-ATP applied to the substrate, the measured Raman intensity, corresponding amount of 4-ATP powder, and laser spot size (1.3 μm), the EF is calculated to be approximately 2.8×10^{7}.

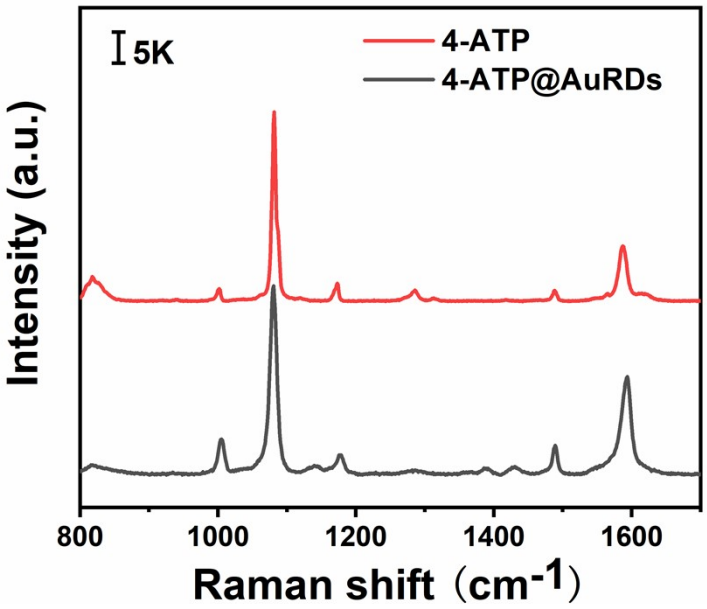

Fig. S11 Raman spectra of 4-ATP powder with the number of molecules $N_{RS}=6\times10^{11}$, and the SERS spectra of 4-ATP on the Au RDs substrates, with estimated number of molecules $N_{4\text{-}ATP}=2\times10^{4}$.

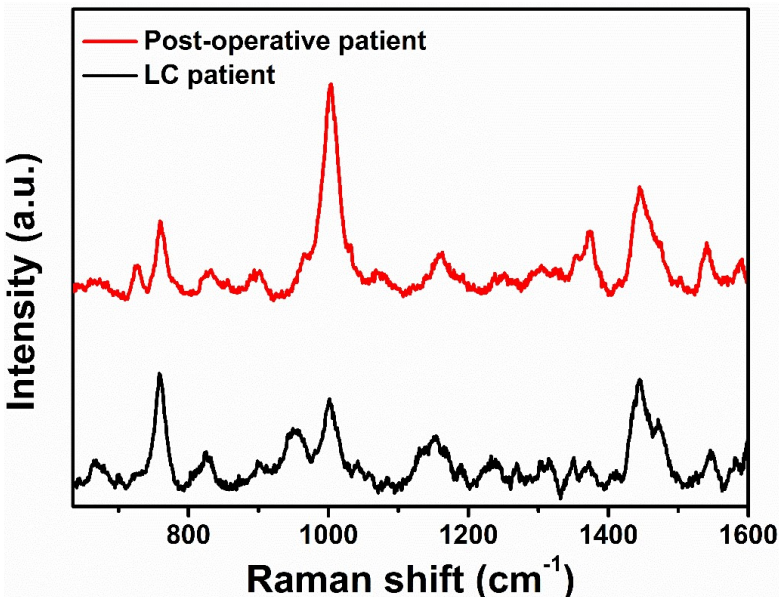

Fig. S12 SERS spectra obtained from a same LC patient diagnosed with minimally invasive adenocarcinoma before (black curve) and after surgery (red curve).

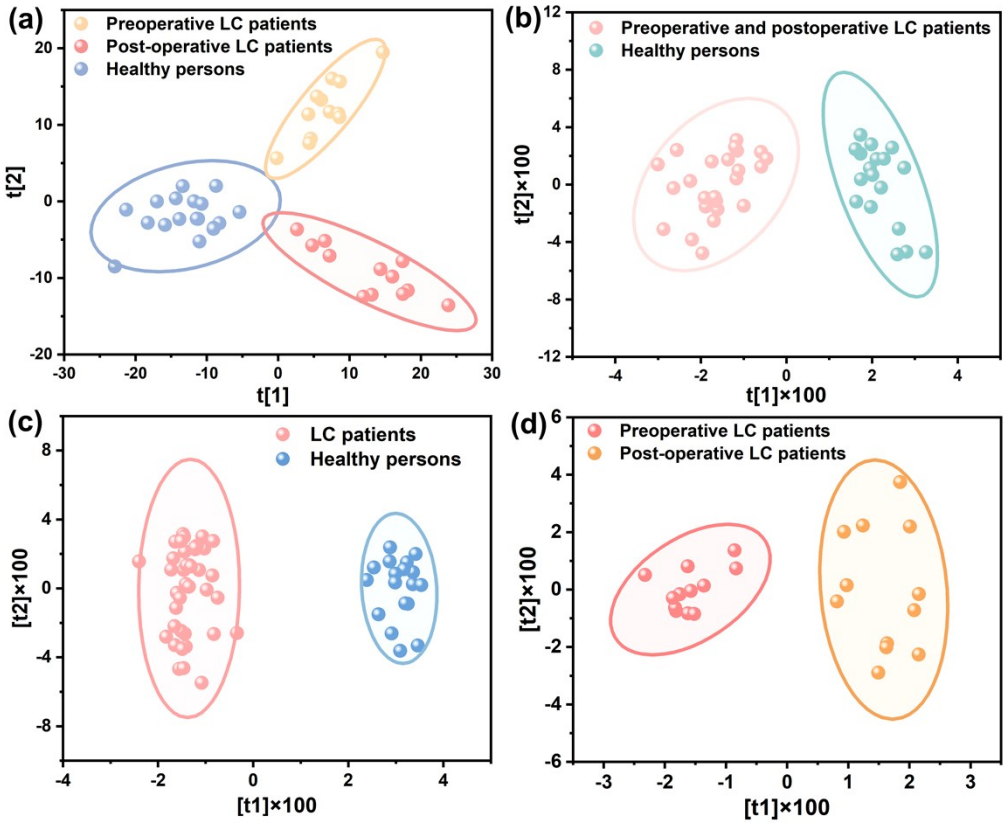

Fig. S13 The OPLS-DA plot for the urine samples from 12 LC patients before and after operation, and 18 healthy persons (a). The OPLS-DA plot for the urine samples from LC patients (24 preoperative and post-operative LC patients) and 18 healthy persons (b). The OPLS-DA plot for 12 LC patients before and after operation (c). The OPLS-DA plot for 41 LC patients and 18 healthy persons (d).

Table S1 Clinical characteristics of the studied samples in this work

Sample	State	Age	Gender	Characteristics	Size of nodules (cm*cm)	Number of nodules	CEA (μg/L)	Keratin 21-1 (μg/L)	SCCA (μg/L)	Total bilirubin(μmol/L)	Direct bilirubin(μmol/L)	Urea/Creatine	Blood urea nitrogen (mmol/L)	Creatine (μmol/L)
1#	Preoperation	40	Female	Adenocarcinoma	0.8*0.8	1	2.4	1.7	0.9	17	5	13.8	3.8	68
2#	Preoperation	51	Female	Minimally invasive adenocarcinoma	1.6*1.1	1	0.6	0.8	0.4	9	3	22.9	5	54
3#	Preoperation	57	Female	Invasive adenocarcinoma	2.4*1.5	1	0.7	2.8	0.7	9	3	20.6	6	72
4#	Preoperation	42	Male	Minimally invasive adenocarcinoma	0.8*0.8	1	1.9	2	1	18	6	13.6	4.9	89
5#	Preoperation	51	Female	Adenocarcinoma in situ/ Minimally Invasive adenocarcinoma	1.2*1.2/0.6*0.6	2	0.9	2	1.5	12	3	17.3	3.9	56
6#	Preoperation	60	Female	Minimally invasive adenocarcinoma	*	1	0.7	2	2	13	5	12.6	3.3	65
7#	Preoperation	68	Female	Minimally invasive adenocarcinoma	0.8*0.8	1	1.5	2.7	1.5	6	2	22.1	4.9	55
8#	Preoperation	71	Female	*	*	*	*	*	*	*	*	*	*	*
9#	Preoperation	60	Female	Minimally invasive adenocarcinoma	4*3	1	3.4	3.3	0.9	8	2	26.2	5.4	51
10#	Preoperation	35	Male	*	*	*	*	*	*	*	*	*	*	*
11#	Preoperation	68	Male	*	*	*	*	*	*	*	*	*	*	*
12#	Preoperation	59	Male	Minimally invasive adenocarcinoma	1.3*0.7	1	2.1	2.8	0.7	13	5	22.3	7.1	29
13#	Preoperation	44	Female	Adenocarcinoma in situ	0.5*0.5/0.5*0.5	2	1.6	2.9	4.3	5	2	19	22.2	289
14#	Preoperation	54	Male	Squamous cell carcinoma	*	*	9.19	10.81	14.2	*	*	*	*	*
15#	Preoperation	58	Male	Adenocarcinoma	*	*	15.24	5.34	*	*	*	*	*	*
16#	Preoperation	69	Male	Adenocarcinoma	*	*	119.1	*	*	*	*	*	*	*
17#	Preoperation	64	Female	Adenocarcinoma	*	*	*	*	*	*	*	*	*	*
18#	Preoperation	77	Female	*	*	*	5.61	4.15	*	*	*	*	*	*
19#	Preoperation	60	Female	*	*	*	*	*	*	*	*	*	*	*
20#	Preoperation	74	Male	Squamous cell carcinoma	*	*	*	94.33	*	*	*	*	*	*
21#	Preoperation	44	Male	*	*	*	*	*	*	*	*	*	*	*
22#	Preoperation	69	Male	Adenocarcinoma	*	*	*	4.59	*	*	*	*	*	*
23#	Preoperation	47	Male	*	*	*	12.87	8.81	1.9	*	*	*	*	*
24#	Preoperation	62	Male	Squamous cell carcinoma	*	*	6.5	33.6	*	*	*	*	*	*
25#	Preoperation	65	Male	Adenocarcinoma	*	*	*	*	*	*	*	*	*	*
26#	Preoperation	57	Male	Invasive adeno carcinoma	*	*	28.4	6.19	*	*	*	*	*	*
27#	Preoperation	66	Male	Squamous cell carcinoma	*	*	*	5.27	*	*	*	*	*	*
28#	Preoperation	65	Male	Adenocarcinoma	*	*	*	*	*	*	*	*	*	*
29#	Preoperation	56	Male	Minimally invasive adenocarcinoma	*	*	*	*	*	*	*	*	*	*
30#	Postoperation	66	Male	*	*	*	*	*	*	*	*	*	*	*
31#	Postoperation	68	Female	*	*	*	3	*	*	6	2	9.9	2.2	55

32#	Postoperation	40	Female	*	*	*	2.7	*	*	11	4	7.7	1.7	47
33#	Postoperation	51	Female	*	*	*	0.8	*	*	8	2	10.5	2	47
34#	Postoperation	60	Female	*	*	*	0.6	2.7	0.7	12	4	14.2	4	70
35#	Postoperation	42	Male	*	*	*	3	*	*	14	6	11.1	5.2	97
36#	Postoperation	57	Female	*	*	*	0.7	*	*	7	2	15.1	3.6	59
37#	Postoperation	51	Female	*	*	*	0.7	*	*	9	3	36.3	6.6	45
38#	Postoperation	60	Female	*	*	*	1.3	1.7	0.5	10	4	27.9	5.4	48
39#	Postoperation	59	Male	*	*	*	1.5	*	1.1	12	4	16	6	93
40#	Postoperation	44	Female	*	*	*	*	*	*	5	2	22.1	13.3	273
41#	Postoperation	*	Male	*	*	*	*	*	*	*	*	*	*	*
42#	Healthy	46	Male	*	*	*	*	*	*	*	*	*	*	*
43#	Healthy	28	Male	*	*	*	*	*	*	*	*	*	*	*
44#	Healthy	44	Female	*	*	*	*	*	*	*	*	*	*	*
45#	Healthy	62	Female	*	*	*	*	*	*	*	*	*	*	*
46#	Healthy	55	Female	*	*	*	*	*	*	*	*	*	*	*
47#	Healthy	43	Female	*	*	*	*	*	*	*	*	*	*	*
48#	Healthy	39	Male	*	*	*	*	*	*	*	*	*	*	*
49#	Healthy	64	Female	*	*	*	*	*	*	*	*	*	*	*
50#	Healthy	72	Male	*	*	*	*	*	*	*	*	*	*	*
51#	Healthy	51	Male	*	*	*	*	*	*	*	*	*	*	*
52#	Healthy	57	Female	*	*	*	*	*	*	*	*	*	*	*
53#	Healthy	49	Female	*	*	*	*	*	*	*	*	*	*	*
54#	Healthy	58	Male	*	*	*	*	*	*	*	*	*	*	*
55#	Healthy	61	Female	*	*	*	*	*	*	*	*	*	*	*
56#	Healthy	54	Male	*	*	*	*	*	*	*	*	*	*	*
57#	Healthy	68	Male	*	*	*	*	*	*	*	*	*	*	*
58#	Healthy	75	Male	*	*	*	*	*	*	*	*	*	*	*
59#	Healthy	48	Female	*	*	*	*	*	*	*	*	*	*	*

* denotes the information that is unavailable. CEA and SCCA are the abbreviations of carcinoembryonic antigen and squamous cell carcinoma antigen, respectively.

Among the 59 research samples, the top 29 were LC patients, the middle yellow part was 12 postoperative LC patients, and the last blue part was 18 healthy individuals. Among them, 29 LC patients mainly had adenocarcinoma (including adenocarcinoma in situ (AIS), minimally invasive adenocarcinoma (MIA), and invasive adenocarcinoma (IAC)) and squamous cell carcinoma.

The 'characteristics' column represents the characteristics of LC patients, while the' Size of nodules' column represents the size of the corresponding patient's nodules. The Number of nodules column is the number of nodules corresponding to the patient. Then, the rest columns are their corresponding concentrations of carcinoembryonic antigen (CEA), Keratin 21-1, and squamous cell carcinoma antigen (SCCA), Total bilirubin, Direct bilirubin, Urea/Creatine, Blood urea nitrogen, and Creatine in serum.

Table S2 Major SERS peaks of urine samples and tentative vibrational mode assignments

Peak position (cm^{-1})	Vibrational modes	Tentative assignments	Reference
660	C-S stretching	Cystine	1,2
685	C-H vibration	Thymidine	3
725	C-H vibration, N-N vibration	Adenosine	3
759	Symmetric breathing	Tryptophan	4
786	Ring breathing mode	Purine nucleoside	3
930~965	Skeletal C-C vibration	Amino acids	1,5
1002	C-C ring stretching/C-N stretching	Amino acids/Urea	6
1082	P-O stretching of HPO_4^{2-}	Phosphorous salts/ phosphodiester groups	1,7
1148	H-C-H twisting and rock	Phenylalanine	3
1270	C-N stretching	Amide	1
1288	C-N stretching	Cytosine	8
1343~1400	Ring breathing/C-H twist vibration/ COO^-	DNA/RNA bases/Amino acids	9,10
1462	C-H bending/C-N stretching	Adenine	4
1542	C=C vibration/NH_2 vibration	Adenosine/ Phenylalanine	3

References

1 Z Movasaghi, S Rehman, IU Rehman, Raman Spectroscopy of Biological Tissues, *Appl. Spectrosc. Rev*, 2007, **42**, 493-541.

2 N Stone, C Kendall, N Shepherd, P Crow, H Barr, Near-infrared Raman spectroscopy for the classification of epithelial pre-cancers and cancers, *J. Raman Spectrosc*, 2002, **33**, 564-573.

3 X Lin, L Wang, H Lin, A novel urine analysis technique combining affinity chromatography with Au nanoparticle based surface enhanced Raman spectroscopy for potential applications in non-invasive cancer screening, *J. Biophotonics*, 2019, **12**, e201800327.

4 N Stone, C Kendall, J Smith, P Crow, H Barr, Raman spectroscopy for identification of epithelial cancers, *Faraday Discuss.*, 2004, **126**, 141-157; discussion 169-183.

5 DP Lau, Z Huang, H Lui, Raman spectroscopy for optical diagnosis in normal and cancerous tissue of the nasopharynx—preliminary findings, *Lasers in Surgery and Medicine*, 2003, **32**, 210-214.

6 E Ó Faoláin, MB Hunter, JM Byrne, A study examining the effects of tissue processing on human tissue sections using vibrational spectroscopy, *Vib. Spectrosc*, 2005, **38**, 121-127.

7 E Gazi, J Dwyer, P Gardner, Applications of Fourier transform infrared microspectroscopy in studies of benign prostate and prostate cancer. A pilot study, *J. Pathol*, 2003, **201**, 99-108.

8 AJ Ruiz-Chica, MA Medina, F Sánchez-Jiménez, FJ Ramírez, Characterization by Raman spectroscopy of conformational changes on guanine–cytosine and adenine–thymine oligonucleotides induced by aminooxy analogues of spermidine, *J. Raman Spectrosc.*, 2004, **35**, 93-100.

9 I Notingher, C Green, C Dyer, Discrimination between ricin and sulphur mustard toxicityin vitrousing Raman spectroscopy, *J. R. Soc. Interface* 2004, **1**, 79-90.

10 G Shetty, C Kendall, N Shepherd, N Stone, H Barr, Raman spectroscopy: elucidation of biochemical changes in carcinogenesis of oesophagus, *J. Cancer*, 2006, **94**, 1460-1464.